

A Novel Peak Torque Excitation Technique for Torque Improvement in Exterior Rotor Permanent Magnet Brushless DC Motor

Dr.K.Uma devi¹, Dr.R.Satish kumar²

¹Assistant Professor,EEE Department, Sengunthar Engineering College,Tiruchengode,India

² Assistant Professor,EEE Department, Sengunthar Engineering College,Tiruchengode,India

Abstract— *A novel excitation technique has been proposed for Exterior Rotor Permanent Magnet Brushless Direct Current (ERPMBLDC) Motor to improve its torque. In this work three phase windings of the stator of ERPMBLDC motor have been not only excited according to the rotor positions but also at phase angles corresponding to peak torque. Flux pattern, phase angles for maximum torque and torque were identified through simulation of ERPMBLDC motor by using Finite Element Method Magnetic 4.2(FEMM4.2) software. A prototype model has been developed to corroborate simulation results and good agreement has been found.*

Keyword- *Exterior Rotor Permanent Magnet Brushless DC Motor (ERPMBLDCM), Finite Element Method (FEM), Flux, Magnetic Vector Potential and Torque.*

I. INTRODUCTION

Conventional DC machines excited by field windings are largely being replaced by low cost permanent magnet DC machines developed by Campbell [19]. This development is mainly due to the availability of low cost high energy permanent magnets as they can be used for replacing the bulky wound field excitation and its associated losses in conventional DC machines.

AC motors using permanent magnets are being used increasingly in modern speed and position control applications used [20]. The main advantages of these motors include high power-to-weight ratio, high torque to the current ratio, fast dynamic response, high power factor and minimal maintenance compared with the conventional motors. The usage of permanent magnet brushless AC (PMBLAC) and permanent magnet brushless DC (PMBLDC) drives for many applications, ranging from servos to traction drives have been increasing nowadays [7] and [4]. They differ primarily in their current and Back-Electromotive-force (EMF) waveforms. It is desirable for a PMBLAC motor to have a sinusoidal back-EMF waveform and PMBLDC motor to have a trapezoidal back-EMF waveform in order to minimize the torque ripple and maximize the efficiency and torque capability. Because of this very reason trapezoidal PMBLDC motor has been chosen for the proposed work.

Two types of sensorless control topologies of BLDC motors has been discussed [21]-[24]. The first topology is the position sensing using the back EMF of the motor, and the second topology is position estimation using motor parameters. The second type usually needs complicated computation, and the cost of the system is relatively high.

Torque calculation for brush less alternating current motor based on Maxwell stress theory and the filtered contributions due to the harmonics of the magnetic vector potential in the motor air gap have been found [3]. These methods lead to simplification in the average torque calculation. The zero crossing points of back -EMF were used for generating proper commutation control of inverter by sampling the voltage of floating phase [12]. The same technique has been used in this proposed work for obtaining rotor positions. Finite Element Method (FEM) over the analytical approach to permanent magnet (PM) motors is the inherent ability to calculate accurately armature reaction effects, inductances and the electromagnetic torque variation with rotor position which was discussed [18].

FEM and Maxwell's stress tensor in cylindrical co-ordinates have been used to analyze magnetic flux density, the magnetic force and the torque in a 3D BLDC motor [8]. A new torque control algorithm for 3 phase BLDC motors to get maximum torque in the high speed region has been proposed. Here it has been advanced the phase angle of stator phase current to match with back EMF for the torque maximization only in the high speed region [1],[6]. A simplified modeling and experimental analysis of Permanent Magnet Brushless DC (PMBLDC) motors for Sensorless operation using Matrix Laboratory (MATLAB) has been proposed. This model provides a mechanism for monitoring and controlling the voltage, current, speed and torque response. They have analyzed Direct torque control (DTC) switching technique of BLDC motor for propulsion system and simulated in MATLAB [5],[17]. Now based on the literature study, here it has been proposed concept of Peak Torque Excitation (PTE) technique to improve the torque of ERPMBLDC motor without any additional hardware components to its drive circuit.

II. MODELING AND SIMULATION OF EXTERIOR ROTOR PERMANENT MAGNET BRUSHLESS DIRECT CURRENT (ERPMBLDC) MOTOR

The purpose of this chapter is to investigate the Finite Element Modeling of ERPMBLDC motor by proposed Peak Torque Excitation (PTE) technique. FEM is a numerical technique for solving problems with complicated geometries, loadings and material properties where analytical solutions cannot be easily obtained. The basic concept is to model a body or structure by dividing it into smaller elements called "Finite Elements", interconnected at points common to two or more elements (nodes). The properties of the elements are formulated as equilibrium equations. The equations for the entire body are then obtained by combining the equilibrium equation of each element such that continuity is ensured at each node. The necessary boundary conditions are then imposed and the equations of equilibrium are then solved to obtain the required variables.

A. ALGORITHM

FEMM4.2 software has been used for modelling and simulating the ERPMBLDC motor with Peak Torque Excitation technique which has been proposed in this thesis. The algorithm for this is given below.

1. Stator is given with a three phase supply.
2. Rotor is rotated from 0 to 87.5 degree with 2.5 degree as periodic interval.
3. At every rotation,
 - a. Phase angle (θ) is noted using the formula
$$\theta = (K * 5 * (3.14)) / 180. \quad (1)$$
Where, θ = Phase angle in degree
K = constant
 - b. The phase angle K varies from 0 to 72 serially to have 73 iterations to increase the accuracy of system.
 - c. The torque value against each phase angle is noted and the phase angle which yields maximum torque is identified.
 - d. Triggering instants for Prototype are identified from the torque values and the corresponding phase angles.
4. The torque values of proposed work are to be compared with the conventional method.

B. ERPMBLDC MOTOR FIELD COMPUTATIONS AND SOLUTION

Vector magnetic potential is of great value when solving two-dimensional problems containing current carrying areas used [25]. This equation is reformulated by variational calculus, in the finite element method, and first-order triangular elements are used to discretize the field region, resulting in a set of linear algebraic equations proposed [26]. These linear simultaneous equations are solved using Newton-Raphson technique to obtain the magnetic vector potential.

FEMM4.2 is a suite of programs for solving low frequency electromagnetic problem on two-dimensional planar and axisymmetric domains. This motor model was developed by using AUTO CAD and exported to the software FEMM4.2 procedure for implementing this numerical computation of magnetic field problems is by using the finite element method which is divided into three main steps.

The three main steps consisting:

1. Pre - processing
2. processing
3. Post - processing

1). Pre-Processing

This pre-processing is used for drawing the problems in geometry, defining materials and defining boundary conditions. The derivation of the finite element model of ERPMBLDC motor under consideration involves defining conduction materials, electromagnetic materials and their properties and boundary conditions and eventually results in mesh generation. The material's properties and boundary conditions are input into various defined region/section of the computational space.

2). Processing

Solving the problem by the relevant Maxwell's equations and obtaining the field distribution in the analyzed domain of the geometry for the ERPMBLDC Motor at arbitrarily chosen excitations and loading conditions, is designed to get the flux and torque pattern.

This section of FEMM is used to view the solutions generated by FEMM4.2 solver. This is the process of calculating and presenting an ERPMBLDC Motor flux pattern and deducing results as well as parameters from the analyzed model. The finite element analysis allows for fast parameterization to scrutinize and to manipulate the number of segments on the magnetic flux density distribution.

3) Post- Processing

The three phase stator windings are excited by three phase currents namely A,B and C by varying the phase angles from 0⁰-360⁰ with interval of 5 i.e. in total 73 iterations for each rotor position. The torque values corresponding to the phase angles are investigated. This procedure is repeated for rotor angles from 0⁰- 90⁰ with an increment of 2.5⁰. Torque for various phase angles from 0⁰-360⁰ for rotor from starting position at 00⁰ to 87.5⁰ has been graph depicted. For each rotor position peak torque value is determined and in total 36 rotor positions are studied for one quadrant.

C. MATHEMATICAL MODELING FOR MAGNETIC TORQUE CALCULATION

The characteristic shape of the back-EMF of the BLDC motor is trapezoidal. This is in contrast with the PMSM, which has a sinusoidal back-EMF. The windings are wound in a different fashion to obtain such a result. The control of a BLDC motor is based on using only the flat portion of the back-EMF in combination with rectangular shaped currents to produce torque [28]. The torque of permanent magnet motors can be determined analytically or numerically. The accuracy of the analytical methods depends on the assumptions made. Some analytical models of torque calculation ignore the core saturation, while in fact saturation widely exists in PM motors. Analytical torque calculation is only fit for machines with simple geometries [29]. Numerical calculation methods of torque can be used for complex geometries and it takes into account saturation. The Finite Element Method (FEM) is a powerful and effective tool to numerically determine the torque for permanent magnet motors. The three most common numerical methods for torque calculation are Maxwell stress tensor method, co-energy method and Coulomb virtual work method [27]&[30]. Maxwell stress tensor method is used to determine the torque here. The use of the Maxwell stress tensor is simple from a computational perspective, since it requires only the local flux density distribution along specific line or contour. Using the definition of Maxwell stress tensor, the electromagnetic forces can be determined on the basis of the magnetic flux density [31].

The total force

$$\vec{F} = \iint_S \left[\frac{1}{\mu_0} \vec{B} (\vec{B} \cdot \vec{n}) - \frac{1}{2\mu_0} B^2 \vec{n} \right] dS \quad (2)$$

The normal force

$$F_n = \frac{L_i}{2\mu_0} \oint_{\Gamma} [B_n^2 - B_t^2] dl \quad (3)$$

The tangential force

$$F_t = \frac{L_i}{\mu_0} \oint_{\Gamma_i} B_n - B_t dl \quad (4)$$

where

- \vec{n} = The normal vector to \vec{B}
- L_i = Stack length
- l = Integration contour
- B_n = Radial (Normal) component to the magnetic flux density
- B_t = Tangential component of the magnetic flux density

The torque

$$\vec{T} = \vec{r} \times \vec{F} \quad (5)$$

r = The air gap radius.

Since radial flux permanent magnet motors can be modeled in 2D, Equation (3.41) can be simplified to line integration along a closed contour Γ in the air gap. This has the benefit of quick calculations.

$$T = \frac{L_i}{\mu_0} \oint r B_n B_t dl \quad (6)$$

Since a finite grid is being used the above equations can be written for element i . The torque shown below in cylindrical coordinates is a sum of torques for each element i , i.e.,

$$T = \frac{L_i}{\mu_0} \sum r^2 \int_{\theta_i}^{\theta_{i+1}} B_{\gamma i} B_{\theta i} d\theta \quad (7)$$

The accuracy of this method is markedly dependent on the model discretization and on the selection of the integration line or contour. The Maxwell stress tensor line integration necessitates a precise solution in the air gap, demanding a fine discretization of the model in the air gap since the flux density is not continuous at the nodes and across boundaries of first-order elements [33].

When the situation becomes more complicated, this ordinary procedure can become impossibly difficult with equations spanning multiple lines. It is therefore convenient to collect many of these terms in the Maxwell stress tensor and to use tensor arithmetic to find the answer to the problem at hand. The torque derived from this method depends on the accuracy of the flux densities and the selection of the integration contour [32].

D. SIMULATION RESULTS FOR ERPMBLDC MOTOR

Figure 1 shows Phase angle Vs torque for three rotor position angles that is for 00° , 2.5° and 5° . Maximum torques and corresponding phase angles are noted for each rotor position. They are 0.01511N-M and 270.246° for rotor angle 00° , 0.07868 N-M and 300.273° for rotor angle 2.5° and 0.03765 N-M and 310.282° for rotor angle 5° respectively. Reading recorded from simulation results for these rotor positions have been shown in Appendix A.1.

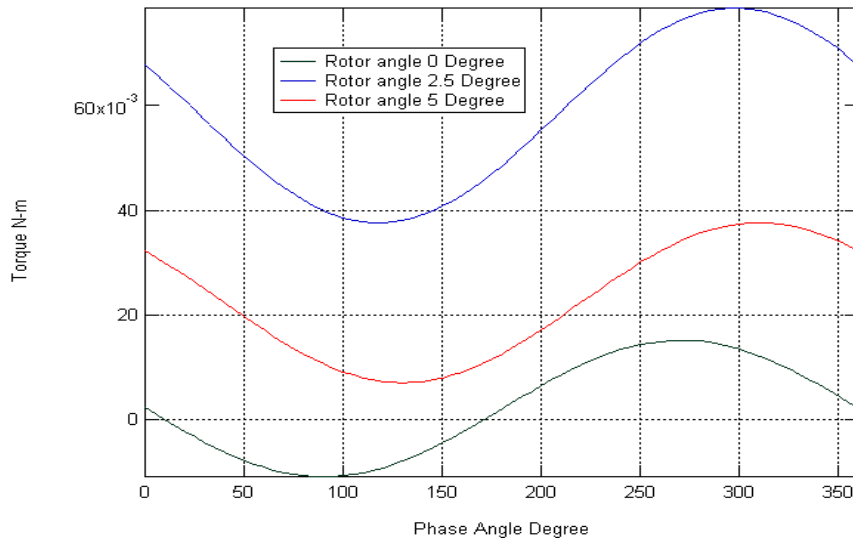


Figure 1 Torque for various rotor position angles (00° to 5°)

Figure 2 shows plot between Peak torque for various rotor position angles in both positive and negative values. Either positive or negative values are to be considered to run the ERPMBLDC motor in either forward or reverse direction respectively. Torque values for various phase angles are plotted at different rotor positions.

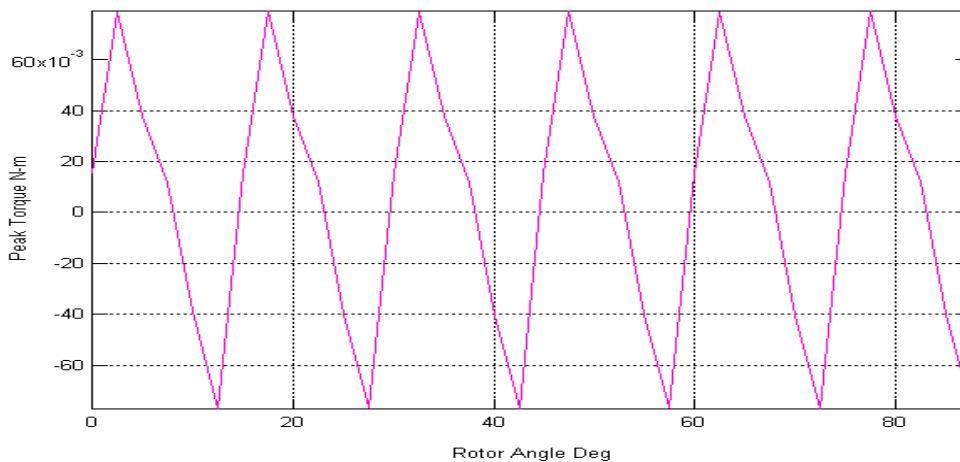


Figure 2 Peak torque for various rotor position angles

It is observed from the plot that the torque developed by the ERPMBLDC motor can be improved to approach the maximum torque by designing the switching circuit suitably motor to supply the phase current to develop the maximum torque for particular rotor positions. The torque developed will be the maximum for the particular motor and hence the output power.

III. HARDWARE IMPLEMENTATION OF ERPMBLDC MOTOR

In the last two decades, permanent-magnet brushless DC (PMBLDC) motors have widely used in various small-size and low-cost drives. Efficiency of electronically controlled drive for electrical machines was improved due to the development in power electronics, digital electronics and electrical machine design in the last decade. Nowadays digital control systems are continuing to replace classical analog control by using fast numerical computing microprocessors and microcontrollers. A microcontroller based experimental set up has been constructed to impalement Peak Torque Excitation (PTE) technique.

A. PEAK TORQUE EXCITATION TECHNIQUE

Peak Torque Excitation technique has been implemented here in a prototype model to experiment its reliability. An experimental circuit has been constructed for an eight pole ERPMBLDC motor by using inverter circuit, Microcontroller, inverter driver circuit and signal conditioning circuit.

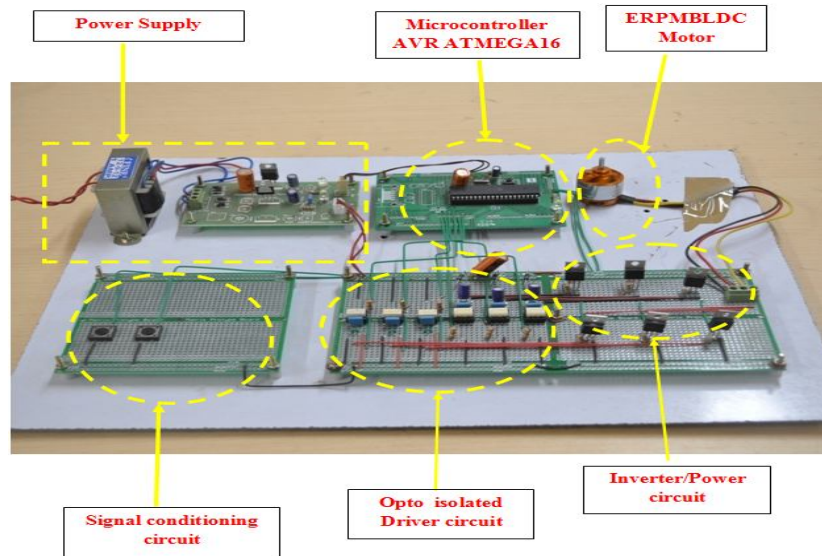


Figure 3. Photograph of ERPMBLDC Motor driver circuit

PTE technique is to excite the motor stator windings at phase angles corresponding to maximum torque for each rotor position. The phase angles predetermined by simulation have been used here to implement PTE technique. An ATMEGA16 microcontroller has been programmed to excite the three phase stator windings through MOSFET based inverter circuit at predetermined phase angles. MOSFETs are triggered by TLP250 MOSFET drivers which are controlled by the microcontroller. The motor is running at maximum possible torque at particular rotor position due to PTE technique.

Figure 3 shows photograph of ERPMBLDC Motor driver circuit. Its voltage, current and power rating are 10.8 Volts, 13 Amperes and 150 Watts respectively. The motor is a miniature ERPMBLDC motor. The most efficient method of controlling the output voltage is to incorporate PWM control within the inverters. In this method a fixed DC input voltage is supplied to the inverter and a controlled AC output voltage is obtained by adjusting the on and off periods of the inverter devices.

IV. RESULTS AND DISCUSSION

The proposed model uses multiple pulse width modulation (MPWM). MOSFETS are driven by TLP250 MOSFET drivers. In this circuit at any movement MOSFETS in two phases are carrying excitation signal for stator winding and rest one is carrying back EMF signal. The back EMF signal are controlled and given to the microcontroller ATMEGA16. Based on the received back EMF signals the microcontroller generates six driver signals to drivers.

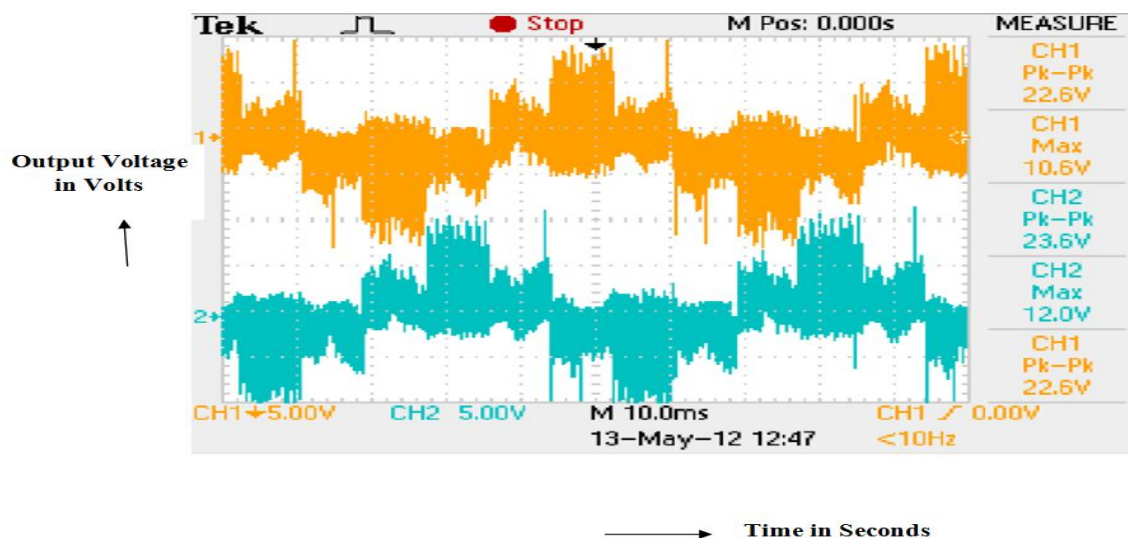


Figure 4 Output Voltage of power circuit (V_{RY} phase-phase) by proposed method

In this model at any time two conducting phases are used for exciting the stator winding to run the rotor in forward direction at possible peak torque by sensor less control. Here the non conducting phases are used for obtaining back EMF signal to identify rotor position. It is possible to determine when to commutate the motor drive voltages by sensing the back EMF voltage on floating motor terminal (phase). The obvious cost advantage of sensor less control is the elimination of the Hall position sensors.

Figure 4 shows R phase to Y phase voltage ($V_{RY \text{ phase-phase}}$) in output of power circuit by proposed method implemented in hardware circuit. This voltage is measured in order to calculate the developed torque.

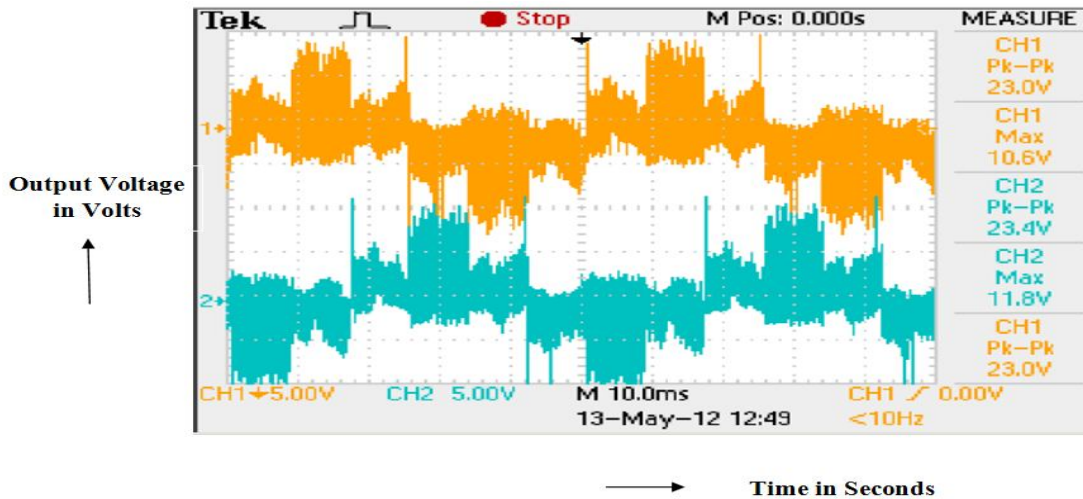


Figure 5. Output Voltage of power circuit ($V_{YB \text{ phase-phase}}$) by proposed method

Figure 5 shows in Output of power circuit ($V_{YB \text{ phase-phase}}$) for Y phase to B phase voltage by proposed method. Torque developed by the proposed technique as noted from the Figure 4 and 5 are made using in the following equations to calculate Peak Torque.

$$\text{Peak Torque} = (I \times K_t) \text{ in N-M} \quad (8)$$

Where,

$$\begin{aligned} \text{Torque constant } K_t \\ = K_b \times 1.345 \end{aligned} \quad (9)$$

$$\text{Voltage constant } K_b = \frac{\text{Voltage}}{\text{Speed}} \quad (10)$$

Here the non conducting phases are used for obtaining back EMF signal to identify rotor position. It is possible to determine when to commutate the motor drive. Cost advantage of sensorless control is the elimination of the Hall position sensors.

V. COMPARATIVE ANALYSIS

The Table 1 shows Comparison of torque developed by Conventional method, proposed Peak torque method by simulation and proposed Peak torque method by experiment. Previous literatures [34] analyzed the maximum torque of a BLDC motor by advance angle technique that too only in high power regions which contributes less to the average torque development whereas PTE technique has been applied in the entire motor operating regions.

Table 1

Improvement Comparison of torque developed by PTE technique by simulation and PTE technique by experiment

Rotor angle in degree	PTE Technique	
	By Simulation Torque(N-M)	By Experiment Torque(N-M)
0	0.01511	0.0162
2.5	0.07868	0.0796
5	0.03765	0.0396
15	0.01505	0.0170
17.5	0.07909	0.0800
20	0.03771	0.0387
22.5	0.01181	0.0128
30	0.01509	0.0160

32.5	0.0786	0.0796
35	0.03762	0.0386
37.5	0.01159	0.0125
47.5	0.07911	0.0801
50	0.03771	0.0387
52.5	0.0118	0.0128
60	0.01512	0.0161
62.5	0.07869	0.0796
65	0.03766	0.0386
75	0.01501	0.0160
77.5	0.07901	0.0800
80	0.03766	0.0386
82.5	0.01178	0.0127

VI. CONCLUSION

Phase angles corresponding to peak torque at different rotor positions had been found by simulating the motor model by using software FEMM4.2. The proposed PTE (Peak Torque Excitation) technique has been simulated by using FEMM4.2. It yields the maximum torque for any rotor position. A prototype model was developed and Results obtained from simulation study and experimental works have been compared and they are having good agreement.

APPENDIX 1

TORQUE FOR VARIOUS PHASE ANGLES AT DIFFERENT ROTOR POSITIONS

A .1 TABULATION OF TORQUE FOR VARIOUS PHASE ANGLES AT DIFFERENT ROTOR POSITIONS (00⁰, 2.5⁰ AND 5⁰)

00 Rotor position (Degree)		2.5 Rotor position (Degree)		5 Rotor position (Degree)	
Phase angles (Degree)	Torque (N-M)	Phase angles (Degree)	Torque (N-M)	Phase angles (Degree)	Torque (N-M)
0	0.002135	0	0.067723	0	0.032165
5.00455	0.000997	5.00455	0.0661	5.00455	0.031103
10.0091	-0.00013	10.0091	0.064416	10.0091	0.029974
15.01365	-0.00125	15.01365	0.062684	15.01365	0.028787
20.0182	-0.00234	20.0182	0.060917	20.0182	0.02755
25.02275	-0.00339	25.02275	0.059129	25.02275	0.026274
30.0273	-0.0044	30.0273	0.057333	30.0273	0.024968
35.03185	-0.00537	35.03185	0.055543	35.03185	0.023642
40.0364	-0.00628	40.0364	0.053773	40.0364	0.022305
45.04095	-0.00712	45.04095	0.052036	45.04095	0.020969
50.0455	-0.00789	50.0455	0.050346	50.0455	0.019643
55.05005	-0.00859	55.05005	0.048715	55.05005	0.018337
60.0546	-0.00921	60.0546	0.047155	60.0546	0.017062
65.05914	-0.00974	65.05914	0.045679	65.05914	0.015826
70.06369	-0.01018	70.06369	0.044297	70.06369	0.014641
75.06824	-0.01053	75.06824	0.043021	75.06824	0.013513
80.07279	-0.01078	80.07279	0.04186	80.07279	0.012453
85.07734	-0.01094	85.07734	0.040823	85.07734	0.011468
90.08189	-0.011	90.08189	0.039918	90.08189	0.010566
95.08644	-0.01095	95.08644	0.039151	95.08644	0.009753
100.091	-0.01081	100.091	0.038529	100.091	0.009036
105.0955	-0.01057	105.0955	0.038056	105.0955	0.00842
110.1001	-0.01023	110.1001	0.037735	110.1001	0.00791
115.1046	-0.0098	115.1046	0.037571	115.1046	0.00751
120.1092	-0.00928	120.1092	0.037562	120.1092	0.007222

00 Rotor position (Degree)		2.5 Rotor position (Degree)		5 Rotor position (Degree)	
Phase (Degree)	angles (N-M)	Phase (Degree)	angles (N-M)	Phase (Degree)	angles (N-M)
125.1137	-0.00867	125.1137	0.03771	125.1137	0.00705
130.1183	-0.00798	130.1183	0.038014	130.1183	0.006994
135.1228	-0.00722	135.1228	0.038471	135.1228	0.007054
140.1274	-0.00638	140.1274	0.039078	140.1274	0.007231
145.1319	-0.00548	145.1319	0.039829	145.1319	0.007523
150.1365	-0.00452	150.1365	0.04072	150.1365	0.007928
155.141	-0.00351	155.141	0.041744	155.141	0.008442
160.1456	-0.00246	160.1456	0.042892	160.1456	0.009062
165.1501	-0.00138	165.1501	0.044156	165.1501	0.009783
170.1547	-0.00027	170.1547	0.045527	170.1547	0.010599
175.1592	0.000861	175.1592	0.046994	175.1592	0.011505
180.1638	0.001999	180.1638	0.048545	180.1638	0.012493
185.1683	0.003137	185.1683	0.05017	185.1683	0.013556
190.1729	0.004267	190.1729	0.051855	190.1729	0.014686
195.1774	0.005381	195.1774	0.053587	195.1774	0.015874
200.182	0.006469	200.182	0.055355	200.182	0.017111
205.1865	0.007524	205.1865	0.057143	205.1865	0.018388
210.1911	0.008536	210.1911	0.058939	210.1911	0.019695
215.1956	0.0095	215.1956	0.060728	215.1956	0.021021
220.2002	0.010407	220.2002	0.062498	220.2002	0.022358
225.2047	0.01125	225.2047	0.064234	225.2047	0.023694
230.2093	0.012023	230.2093	0.065924	230.2093	0.02502
235.2138	0.012721	235.2138	0.067555	235.2138	0.026326
240.2184	0.013337	240.2184	0.069113	240.2184	0.027601
245.2229	0.013867	245.2229	0.070588	245.2229	0.028835
250.2275	0.014308	250.2275	0.071968	250.2275	0.03002
255.232	0.014655	255.232	0.073243	255.232	0.031147
260.2366	0.014906	260.2366	0.074402	260.2366	0.032206
265.2411	0.015059	265.2411	0.075437	265.2411	0.03319
270.2457	0.015113	270.2457	0.076341	270.2457	0.034091
275.2502	0.015068	275.2502	0.077105	275.2502	0.034902
280.2548	0.014924	280.2548	0.077725	280.2548	0.035618
285.2593	0.014681	285.2593	0.078196	285.2593	0.036232
290.2639	0.014343	290.2639	0.078514	290.2639	0.036741
295.2684	0.013911	295.2684	0.078676	295.2684	0.037139
300.273	0.013389	300.273	0.078682	300.273	0.037425
305.2775	0.01278	305.2775	0.078532	305.2775	0.037596
310.2821	0.01209	310.2821	0.078226	310.2821	0.03765
315.2866	0.011323	315.2866	0.077766	315.2866	0.037588
320.2912	0.010486	320.2912	0.077158	320.2912	0.037409
325.2957	0.009585	325.2957	0.076404	325.2957	0.037115
330.3003	0.008626	330.3003	0.075511	330.3003	0.036709
335.3048	0.007617	335.3048	0.074486	335.3048	0.036193
340.3094	0.006566	340.3094	0.073335	340.3094	0.035572
345.3139	0.005481	345.3139	0.07207	345.3139	0.034849

00 Rotor position (Degree)		2.5 Rotor position (Degree)		5 Rotor position (Degree)	
Phase angles (Degree)	Torque (N-M)	Phase angles (Degree)	Torque (N-M)	Phase angles (Degree)	Torque (N-M)
350.3185	0.004369	350.3185	0.070697	350.3185	0.034031
355.323	0.00324	355.323	0.069229	355.323	0.033124
360.3276	0.002102	360.3276	0.067677	360.3276	0.032135

Note: Peak torque values are shown **BOLD**

REFERENCES

- [1] Won-Sang Im, Jong-Pil Kim, Jang-Mok Kim, and Kwang-Ryul Beak, "Torque Maximization Control of 3-Phase BLDC Motors in the High Speed Region", Journal of Power Electronics, Vol. 10, No. 6, November 2010
- [2] Bentouati, S., Zhu, Z.Q. and Howe, D. "Influence Of Design Parameters On The Starting Torque of a Single-Phase PM Brushless DC Motor", IEEE Transactions On Magnetics, Vol. 36, No. 5, September 2000.
- [3]. Dan Ionel, M., Mircea Popescu, Malcolm McGilp, I. Miller, T. J. E. and Stephen Dellinger, J. "Assessment of Torque Components in Brushless Permanent-Magnet Machines Through Numerical Analysis of the Electromagnetic Field", IEEE Transactions On Industry Applications, Vol. 41, No. 5, 2005.
- [4]. Hendershot, J. R. and Miller, T. J. E. "Design of Brushless Permanent- Magnet Motors", Oxford, U.K. Magana Physics/Clarendon, 1994.
- [5] Kaliappan, E. and Chellamuthu, C. "Simplified Modeling, Analysis and Simulation of Permanent Magnet Brushless Direct Current Motors for Sensorless Operation", American Journal of Applied Sciences 9 (7): 1046-1054, 2012.
- [6] Kaliappan, E. and Sharmeela, C. "Direct Torque Control of PMLDC Motor using Hybrid (GA and Fuzzy logic) Controller", Journal Of Advances In Information Technology, Vol. 1, No. 4, November 2010.
- [7] Kenjo, T. and Nagamori, S. "Permanent-Magnet and Brushless DC Motors", Oxford, U.K. Clarendon, 1985.
- [8] Majid Pakdel, "Analysis of the Magnetic Flux Density, the Magnetic Force and the Torque in a 3D brushless DC motor", J. Electromagnetic Analysis & Applications, February 2009.
- [9] Miller, T.J.E. "Brushless Permanent-Magnet and Reluctant Motor Drives", Oxford, 1989.
- [10] Rajashekara, K. and Kawamura, A. "Sensorless Control of AC Motor Drivers", IEEE press, 1996.
- [11] Tashakori, A. and M. Ektesabi, A. "Direct Torque Controlled Drive Train for Electric Vehicle", Proceedings of the A. e World Congress on Engineering 2012 Vol. II WCE 2012, July 4 - 6, 2012, London, U.K.
- [12] Yen-shin Lai, and Yong -Kai Lin, "Novel Back -EMF Detection Technique of Brushless DC Motor Drives for Wide Range Control without Using Current and Position Sensors", IEEE Transaction Power Electronics, Vol.23, No.2, March 2008.
- [13] K.Uzuka, H.Uzhashi, et al., "Microcomputer Control for Sensorless Brushless Motor," IEEE Trans. Industry Application, vol.IA-21, May-June, 1985.
- [14]. R.Becerra, T.Jahns, and M.Ehsani, "Four Quadrant Sensorless Brushless ECM Drive," IEEE Applied Power Electronics Conference and Exposition 1991, pp.202-209.
- [15] J.Moreira, "Indirect Sensing for Rotor Flux Position of Permanent Magnet AC Motors Operating in a Wide Speed Range," IEEE Industry Application Society Annual Meeting 1994, pp401-407.
- [16]. Y. Kawaguchi, T. Sato, I. Miki, and M. Nakamura, "A reduction method of cogging torque for IPMSM," in Electrical Machines and Systems, 2005, pp. 248-250 Vol. 1.
- [17]. Jacek f. Gieras, permanent magnet motor technology, united technologies research center hartford, connecticut mitchell wing bt cellnet london, united kingdom, marcel dekker New York Basel-2002, design and applications second edition, revised and expanded.
- [18]. Baltzis, K. B. "The FEMM Package: A Simple, Fast, and Accurate Open Source Electromagnetic Tool in Science and Engineering", Journal of Engineering Science and Technology Review, pp 83-89, 2008.
- [19]. Campbell, P. "Permanent Magnet Materials and Their Applications", Cambridge, U.K, Cambridge University Press, pp. 189-200, 1994.
- [20]. Krishnan, R. "Selection Criteria for Servo Motor Drives," in Proc. IEEE IAS Annual Meeting", pp. 301-308, 1986.
- [21]. Chen, C.H. and Cheng, M.Y. "New Cost Effective Sensor Less Commutation Method for Brushless dc Motors without Phase Shift Circuit and Neutral Voltage", IEEE Transactions Power Electronics, Vol. 22, No. 2, pp. 644-653, March 2007.
- [22]. Kim, H.C., Oh, H.S., Kim, J.M. and Kim, C.U. "A Study on the Phase Advance Angle of High Speed Operation for 7 Phase BLDC Motor Drives", Korean, Journal of Electrical Engineering & Technology, Vol. 56, No. 11, pp. 1930-1936, November 2007.
- [23]. Shao, J., Nolan, D., Tessier, M. and Swanson, D. "A Novel Microcontroller Based Sensorless Brushless (BLDC) Motor Drive for Automotive Fuel Pumps," IEEE Transactions on Industry Applications., Vol. 39, No. 6, pp. 1734-1740, Nov./Dec. 2003.

- [24]. Somanatham, R., Prasad, P.V.N. and Rajkumar, A.D. “Modeling and Simulation of Sensorless Control of PMSBLDC Motor using Zero-Crossing Back E.M.F. Detection”, Power Electronics, Electrical Drives, Automation and Motion, International Symposium, pp. 23-26, May 2006.
- [25]. Reece, A.B.J. and Preston, T.W. “Preston Finite Element Methods in Electrical Power Engineering”, Oxford University Press, New York, 2000.
- [26]. Tandon, S.C. Richter, E. and Chari, M.V.K. “Finite Elements and Electrical Machine Design”, IEEE Transactions on Magnetics, MAG, Vol. 1, No. 5, pp.1020-1022, 1980.
- [27]. Kawaguchi, Y., Sato, T., Miki, I. and Nakamura, M. “A Reduction Method of Cogging Torque for IPMSM”, in Electrical Machines and Systems, 2005. ICEMS 2005. Proceedings of the Eighth International Conference on, Vol. 1. pp. 248-250, 2005.
- [28]. Pragasen Pillay and Ramu Krishnan “Modeling, Simulation, and Analysis of Permanent-Magnet Motor Drives, Part I: The Permanent-Magnet Synchronous Motor Drive”, IEEE Transactions on Industry Applications, Vol. 25, No. 2, pp.265-273, March/April 1989.
- [29]. Zhenhong, G., Liuchen, C. and Yaosuo, X. “Cogging Torque of Permanent Magnet Electric Machines: An overview”, in Canadian Conference on Electrical and Computer Engineering, CCECE '09, pp. 1172-1177, 2009.
- [30]. Zhu, Z. Q., Rusangsinchaiwanich, S., Schofield, N. and Howe, D. “Reduction of Cogging Torque in Interior-Magnet Brushless Machines”, IEEE Transactions on Magnetics, Vol. 39, pp. 3238-3240, 2003.
- [31]. Jacek Gieras, F. “Permanent Magnet Motor Technology”, New York 2002.
- [32]. Mizia, J., Adamiak, K., Eastham, A.R. and Dawson, G.E. “Finite Element Force Calculation: Comparison of Methods for Electric Machines”, IEEE Transactions on Magnetics, Vol. 24, pp. 447-450, 1988.
- [33]. Howe, D. and Zhu, Z.Q. “The Influence of Finite Element Discretization on the Prediction of Cogging Torque in Permanent Magnet Excited Motors”, IEEE Transactions on Magnetics, Vol. 28, pp. 1080–1083, 1992.
- [34]. Wen-Sang Im, Jong-Pil Kim, Jang-Mok Kim, and Kwang - Ryul Beak “Torque Maximization Control of 3-Phase BLDC Motors in the High Speed Region”, Journal of Power Electronics, Vol. 10, No. 6, pp.717-723, 2010.